ASPS Conference Proceedings 1: 1223-1229 (2022)

Proceedings of

12th Structural Engineering Convention-An International Event (SEC 2022)

Available at https://asps-journals.com/index.php/acp

Axial Deformation of Shells at Higher Strain Rates using Buckling Initiators

S. Bhutada [1], M.D. Goel [2, *]

[1] Department of Applied Mechanics, Doctoral Research Scholar, Visvesvaraya National Institute of Technology, Nagpur – 440 010, India
[2] Department of Applied Mechanics, Assistant Professor, Visvesvaraya National Institute of Technology, Nagpur – 440 010, India

Paper ID - 090245

Abstract

Deformation mode of cylindrical shells and their peak load reduction is of prime importance in impact damage mechanics. In this study, numerical investigation is carried out for triggering mechanism induced in the thin-walled axially compressed short stubby shells, considering the damage occurred in vehicle crash or in any other protective equipment. The shells are studied for their initial buckling response under varying impact velocities for two different triggering configurations. Explicit simulation is carried out using ABAQUS/Explicit® to study the initial buckling of the shells by modelling Split Hopkinson Pressure Bar (SHPB) test setup. Initially, numerical scheme is validated using previously available study. Present analysis is carried out using diamond shaped triggering notches and these are configured in such a way that the shell will deform in particular buckling mode, under the impact of three different velocities i.e. 9 m/s, 20 m/s and 40 m/s. Effect of these notches and their pattern of arrangement on reduction in peak load and energy absorption characteristics are studied. Moreover, comparison is made between commonly used circular hole and diamond notch type cut-outs, in order to study the effect of above said parameters along with the energy absorbed, energy efficiency and specific energy absorption for the shells considered herein. By numerically impacting the shells in SHPB, it is observed that peak load reduction is higher in diamond notched shells as compared to circular hole shells. This was due to the geometry and size of the cut-outs considered in this study. Parameters like peak collapse load, energy absorbed, energy efficiency along with stress concentration around the notch are also observed and studied in this work in order to observe and compare the two shapes of cut-outs.

Keywords: Cut-out, Diamond-notch, Deformation, Energy absorption, Strain rate, SHPB

1. Introduction

In the study of impact damage mechanics for a vehicle crash, two most important functions to be served by the vehicle are structural integrity which needs to be maintained for safe evacuation of its occupants and reduction in force which is going to be transmitted to the occupants must be large. These functions are served by the structural component of vehicle, which are capable of absorbing high amount of energy. For the purpose of absorbing such a high amount of energy, thin-walled cylindrical shells are most commonly used as an energy absorbing device. During vehicle crash, kinetic energy of vehicle is absorbed by these shells by deforming into several deformation modes and absorbs high amount of kinetic energy, in turn transmitting significantly reduced amount of forces to its occupants. This axial crushing of shells and its energy absorbing characteristics depends on several factors like material property and geometry of shell, impact velocity, type of loading, and strain rate sensitivity of material, etc.

Many studies had been conducted over the years on the axial crushing of these shells and it was mainly observed that the shells deforming into particular mode of deformation possesses particular energy absorption characteristics. These shells under axial compression perform differently in different type of loading, viz. static loading and dynamic loading. Similar research was carried out by Abramowicz and Jones[1-4] on a large number of square and circular tubes by performing numerous static and dynamic experiments. From this, they developed a well-known half-fold length formula for the buckle formation over the tubes. Further, Wang et al. [5] described theory of two critical velocities which governs the mode of deformation of tube either into axisymmetric mode or non-axisymmetric mode. This theory was established by performing experiments on an aluminium alloy shell fixed at one end and impacted by a mass at another end. Langseth and Hopperstad [6] presented a significant effect of inertia on square Al 6060 alloy tubes, which was indicated by the presence of higher dynamic mean force over the static mean force obtained from the axial crushing thus, linking to the inertia effects of shell.

Karagiozova et al. [7-10] carried out detailed research study on the parameters governing the dynamic progressive buckling of shells. Those parameters were inertial effects of striking mass and shell under consideration, stress wave propagation, impact velocity, strain hardening properties, and geometrical properties of the material like aluminium alloy tubes and steel tubes. Further, considering the crashworthiness of vehicles, metallic tubes are provided with buckling triggers. Several studies had been conducted to study the effect of this buckling triggers provided as pre-

*Corresponding author. Tel: +917722043252; E-mail address: mdgoel@apm.vnit.ac.in

Proceedings of the 12th Structural Engineering Convention (SEC 2022), NCDMM, MNIT Jaipur, India| 19-22 December, 2022

Published online: December 19, 2022
doi:10.38208/acp.v1.644

buckle, wall dents, notches, chamfers, and cut-outs, on the buckling phenomenon of tubes, as well as reduction in peak collapse load [11-22]. Gupta and Gupta [14] conducted the series of experiments to study the optimal cut-out size and their position on the collapse of steel and aluminium cylinders. They concluded that the presence of cut-outs triggers the shell to deform at that position and this could help in preventing the global bending mode in long cylinders. Mamalis et al. [16] observed that location of cut-outs dominates the buckling mode of shell rather than the size of cut-outs. Further experimental and numerical studies were conducted on the Split Hopkinson Pressure Bar (SHPB) setup for the dynamic loading on shells. The first experimental study was implemented by Ming et al. [23], while the numerical model was developed by Karagiozova et al. [24] to compare the experimental results of Ming et al. [23]. Further, Goel [25] conducted a numerical investigation, on Al 6063 alloy circular tubes. The study involves single, double and stiffened form of tubes to improve the energy absorption characteristics. He observed that double and stiffened form tubes were absorbing very high amount of energy as compared to the single tube. It also included the empty and foam filled tubes for axial compression under varying loading conditions [26-29]. In year 2016, Sankar et al. [30] studied the effect of multiple circular holes and their arrangement pattern on the initial buckling response, peak load reduction and energy absorption characteristics of stubby Al 6061-T6 alloy shells. The SHPB experimental observations concluded that circular holes and their arrangement pattern were strongly influencing the peak collapse load and deformation mode. Two different sets of cylinders were considered by keeping the equal weight reduction and same net-section perimeter. The numerical results were in good agreement with the experimental results.

In the present study, an attempt is made to numerically investigate the effect of peak collapse load, energy absorption characteristics, energy efficiency on the Al 6061-T6 alloy shells by changing the shape of cut-out from circular-hole to diamond-shape. Comparison was made between the study of Sankar et al. [30] and the present study, to observe the behaviour of two different cut-out shapes in similar configuration based on equal weight reduction criteria. Further, same set of shells was studied under impact of higher strain rates for reduction in peak collapse load and to study the mode of deformation. While doing so, theory of two critical velocities by Wang et al. [5] is also verified. This study is comprised on a series of numerical simulations carried out using a finite element package ABAQUS/Explicit® [31] to study the behaviour of shells and their deformation modes.

2. Specimen Configuration

The thin cylindrical shell used herein is made up of aluminium 6061-T6 alloy material. Cross-sectional shape of shell is considered as circular with 10 mm length, 15 mm outer diameter, and 0.5 mm thickness. These geometrical details are visualized in Fig. 1 below. The circular cross-section is chosen based on the research from earlier studies. Study states that unlike circular shell, square cross-sectional shell deforms up to certain limit and further the folding is prohibited by the ruptured corners of shells, under the action of dynamic loading [32]. The geometry of the shell is decided by considering certain range of L/D ratio for which the shell will deform in to concertina mode. Further, the shell herein is studied for the formation of first buckle only. And, thus the length of the shell required to form a single fold is calculated from the formula mentioned by Abramowicz and Jones [2], as under

$$\frac{H}{R} = 1.73\left(\frac{h}{2R}\right)^{1/2} \tag{1}$$

where, 'H' is the half-fold length (mm), 'R' is the mean radius (mm), and 'h' is the wall thickness (mm) of the shell. The half fold length obtained here is 2.33 mm, and considering the formation of two complete folds, the required length of the tube becomes 9.32 mm, taking it approximately as 10 mm. Three different types of specimens are considered for the study depending on their notch configuration. The diamond-shape notch is designed on the surface of shell along the line of circumference. These diamond-notches are square in shape, tilted at an angle of 45° to the line of circumference of shell, and with width as 2 mm, 3 mm and 4 mm. Effect of each size notch on the buckling behaviour of shell in studied by locating the notches along the mid-length of the shell in a single row. The configuration of these notches on the cylindrical shell are decided by keeping the equal weight reduction in each of the cylinder, also the schematic representation of those shells is shown in Fig. 1.

There were many criteria for the selection of notch configuration for shell with circular hole in the study of Sankar et al. [30], but the configuration with equal weight reduction was the best yielding configuration in terms of

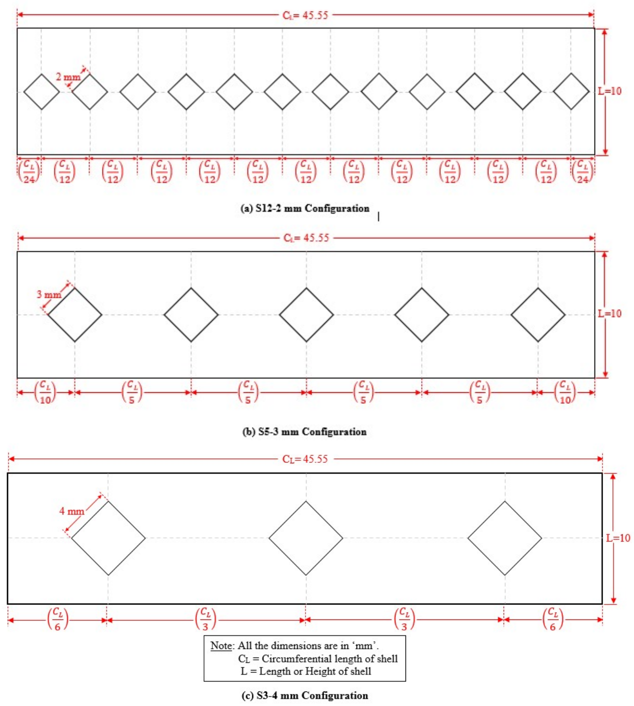

Fig. 1. Location and configurations of notches along the circumference of the shell considered in the present investigation

Table-1. Notch configuration of specimen on the basis of equal weight reduction

Type of notch Configuration	Cylindrical Specimen	Net-Section Perimeter	Weight (g)
S12-2	P1, P4, P7	11.59	0.550
S5-3	P2, P5, P8	24.34	0.554
S3-4	P3, P6, P9	28.57	0.550

Table-2. J-C constitutive model parameters for Al 6061-T6 alloy [33]

Material	*A* (MPa)	*B* (MPa)	*C*	*n*	*m*
Al 6061-T6	324	114	0.002	0.42	1.34

reducing the peak collapse load, without much reduction in the stiffness of the shell. Here, the reduction in weight of the shell was observed to be ~10%. Further geometrical details of these shells, like net-section perimeter and reduced weight, are tabulated in Table 1. The nomenclature decided for the shells with notches is as 'number of holes arranged in a single (S) row-Width of square notch (mm)'.

3. Numerical Simulation Details

3.1 Finite Element (FE) Modelling Details

The explicit finite element simulation for axial compression of shell is carried out using ABAQUS/Explicit®. Complete SHPB setup is modelled to study the deformation and energy absorption characteristics of the shells under consideration. Fig. 2 shows the meshed model developed similar to the experimental setup of SHPB. The cylindrical shell is modelled as S4R element available in ABAQUS/Explicit® element library with deformable properties of shell at each of the 4 nodes of element. The incident bar and transmitter bar of SHPB are modelled as 8-noded brick element with solid deformable properties. The optimised meshing for shell has fifty elements along the length and 200 elements along the circumference of shell. Further, the meshing of incident and transmitter bar of SHPB is done by providing globally seeded elements of 1 mm size in both the direction i.e. longitudinal as well as in circumferential direction. Contact surfaces between bar and shell are defined with a coefficient of friction of 0.25 to maintain the tangential behaviour, while the self-contact between surfaces of shell are assumed to be frictionless

The length of incident and transmitter bars modelled are 3 m and 2 m, respectively, with a diameter of 20 mm each. The material model for bars is isotropic and linearly elastic, with modulus of elasticity of 70 GPa and Poisson's ratio as 0.3. The material of incident and transmitter bars used is aluminium 7075-T6 alloy, with density of 2810 kg/m^3. The geometric details of specimen have already been provided in the earlier section. Herein, shell is modelled using Johnson-

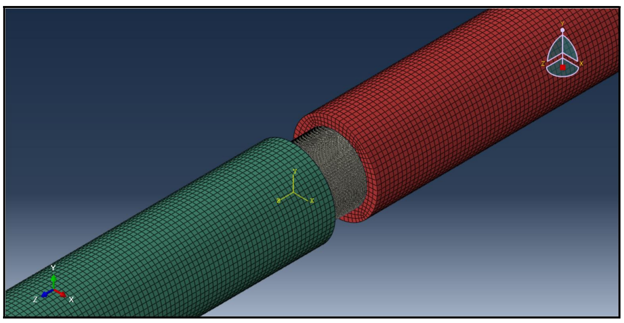

Fig. 2. Meshed model of SHPB setup and specimen for present FE simulation

Cook (J-C) constitutive model, to consider the effect of strain rate in the material. The details of J-C model parameters used for shell material, aluminium 6061-T6 alloy, are provided in Table 2.

3.2 Validation of FE Modelling

The validation for FE modelling is carried out using the experimental and numerical data for cylinder without any holes using the study reported Sankar et al. [30]. The FE material modelling and geometrical as well as physical properties of the specimen are similar to that used by Sankar et al. [30].Fig. 3 shows the nominal stress-strain response of the shell under axial compression impacted by a velocity of around 9 m/s, similar to that used by Sankar et al. [30]. It is observed from this figure that the present numerical scheme and numerical and experimental results of Sankar et al. [30] are in well agreement, thus validating the present numerical scheme. Further, Table 3 shows the results obtained from present FE simulation and results reported by Sankar et al. [30].

Table-3. Parametric results of present FE simulation with Sankar et al. [30]

	Type of Cylinder	σ_{max} (P_{max})	$E_{absorbed}$ (J)	η_{energy} (%)	Specific Energy (kJ/kg)
Sankar et al. [26]	P	344 MPa (7.8 kN)	11.26	47.9	17.9
Present FE Simulation	P	341 MPa (7.76 kN)	12.13	52.1	19.7

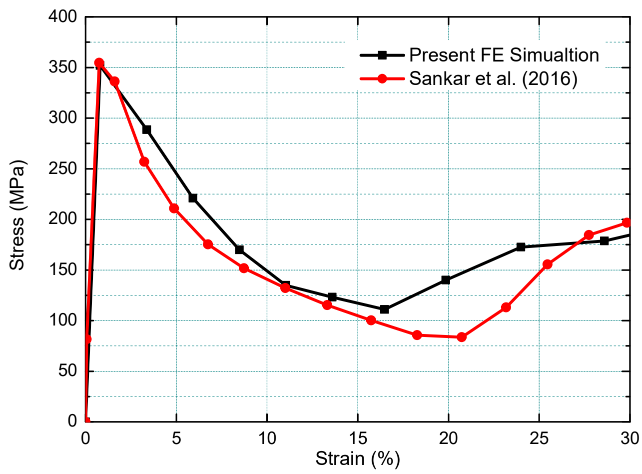

Fig. 3. Validation of the present FE simulation with Sankar et al. [30]

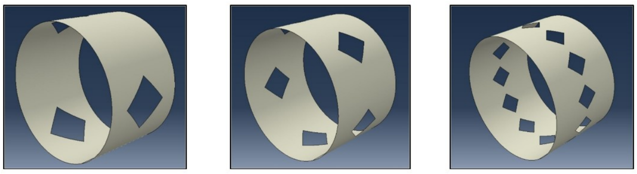

Fig. 4. Modelling of diamond-notched shells in ABAQUS/Explicit®

3.3 FE Simulation of shells with notches

Finite element simulation of shells provided with notches are performed by providing the notches at equidistant along the line of circumference at the mid-length of shell (refer Fig. 1). These notches will trigger the buckling mode of shell under high impact velocity, and then initial buckling response is studied for these shells. The cylindrical shell modelled in earlier section for FE validation is taken and the required number of notches are provided on its surface as per the dimension of notch in each configuration. By doing this, three cylinders are created for each configuration, making in total of nine specimens for the present study. Each specimen is tested at three different velocities viz. 9 m/s, 20 m/s, and 40 m/s, as the velocity changes the strain rate related to velocity also changes. The strain rates corresponding to three velocities are 900 s^{-1}, 2000 s^{-1}, and 4000 s^{-1}, respectively. Further, corresponding to mentioned strain rates, initial buckling response of each shell is studied in terms of different parameters mentioned in section 4. Explicit FE simulation is carried out for all the specimens with defined field outputs like force, displacement, stress, strain, energy absorbed over the specific nodes. Finally, variation of nominal stress with nominal strain is obtained to study the effect of peak collapse load and its reduction simultaneously on each of the notch configuration.

The parameters considered for the thorough numerical investigation of shells with different notches are peak collapse load (P_{max}) and its % reduction as compared to cylinder without notch, energy absorbed ($E_{absorbed}$), energy efficiency (η_{energy}) of the shells under consideration and specific energy absorption (SEA). The complete response of shell during the formation of buckle is evaluated using these parameters, along with the study of stress concentration around the notches. These above said parameters are chosen for a smooth parametric comparison between the cylinder with circular-holes and cylinder with diamond-notches with the results reported by Sankar et al [30].

4. Results and Discussions

4.1 Observation from FE simulations

In the present investigation, axial crushing of cylindrical shells is studied under the influence of three different impact velocities, viz., 9 m/s, 20 m/s, and 40 m/s. This helps to study the deformation pattern and energy absorption characteristics of cylindrical shell at higher strain rates as mentioned earlier. Equal weight reduction criteria are used to prepare the notch pattern on the shell surface. The weight reduction of each shell is ~ 10 %, as compared to the weight of shell without notches.

Table-4. Performance parameters obtained from present FE simulation

Impact Velocity, V_i (m/sec)	Type of Cylinder	σ_{max} (P_{max}) MPa (kN)	$E_{absorbed}$ (J)	η_{energy} (%)	SEA (kJ/kg)
9	P1	186.85 (4.26)	8.7	68.1	15.8
	P2	216.51 (4.93)	8.9	60.2	16.1
	P3	236.93 (5.4)	9.7	59.9	17.6
20	P4	162.50 (3.7)	8.5	76.6	15.5
	P5	202.88 (4.62)	8.4	60.6	15.2
	P6	251.21 (5.72)	9.9	57.7	18.0
40	P7	173.8 (3.96)	8.7	73.2	15.8
	P8	210.65 (4.8)	8.7	60.4	15.7
	P9	246.01 (5.6)	8.7	51.8	15.8

4.2 Parametric Comparison and Discussions

Table 4 summarizes the parameters defined in section 4 for each of the cylinder type. The values obtained in Table 4 are considered only up to axial deformation of 3 mm, or strain of 30%.

The comparison is also made in between the two types of cut-out shapes, viz. circular hole and diamond notch. Fig. 5 shows the bar chart for all the three specimens, tested at same impact velocity of around 9 m/s, for the same trigger configuration with different trigger shape. It can be seen from the bar chart that peak collapse load value is lower for diamond-notch pattern while, reduction in peak collapse load when compared to cylinder without any discontinuity is higher for diamond-notch pattern than circular-hole pattern. As in the case of circular-hole pattern the highest peak load reduction was obtained for 12 numbers of 2 mm circular-hole configuration arranged in single row, similarly for the diamond-notch pattern the highest peak load reduction is observed in same configuration of 12 numbers of 2 mm diamond-notch configuration, but the reduction obtained in the diamond-notch pattern is 6.3% higher than the circular-hole configuration. Similarly, for 3 mm and 4 mm notches, reduction in diamond-notch pattern is 9.8% and 7.7% higher than the circular-hole pattern, respectively (refer Fig. 5). Further, energy efficiency of shell is the ratio of absorbed energy to the product of peak collapse load and deformation (i.e. $P_{max} \times \delta$). And since the peak collapse load obtained for diamond-notch shells is lesser than the circular-hole shells, the energy efficiency is found to be higher for each of the configuration under same impact velocity V_i of 9 m/s. (refer Table 3 and Table 4).

Further, Fig. 6 (a), (b), and (c) represents the comparison of shells with different configurations under three different impact velocities. From Fig. 6(a), for a set of identical specimens P1, P4, and P7, energy absorbed is approximately similar, but the value of peak collapse load is least for the shell P4, leading to the highest peak load reduction among the set considered. This set of specimens, with 2 mm notches, completely deforms into concertina mode of deformation for all the values of impact velocities. And shell P4, is observed to be most energy efficient shell under axial compression, among all other specimens with notches.

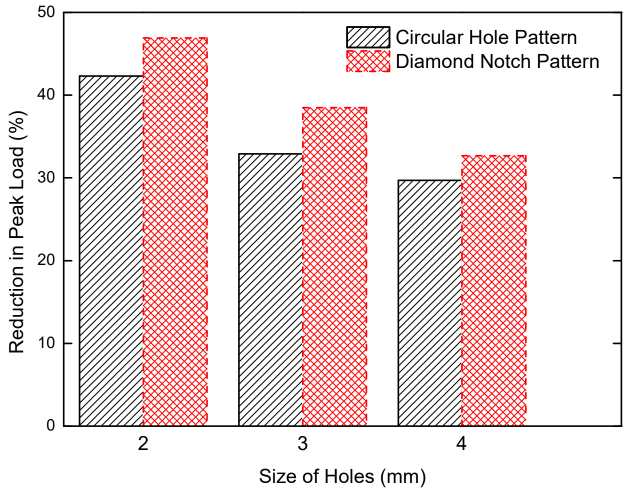

Fig. 5. Comparison of reduction in peak load for circular-hole and diamond-notch pattern having same configuration

Similar behaviour is observed in Fig. 6 (b), for a set of identical specimens P2, P5, and P8, the value of peak collapse load is least and the reduction in peak collapse load is highest in the shell P5. The shell having 5 numbers of 3 mm notches, completely deforms into the pentagonal shape, due to the notches forming 5 edges of pentagon after formation of first buckle completely. The values for these observations can be seen from Table 4. Further, third set of specimens P3, P6, and P9 are observed to behave differently. The least peak load value is obtained under impact velocity, V_i of 9 m/s. Among these 3 shells, shell P9 under impact velocity, V_i of 9 m/s, initially deforms into concertina, then further transition is observed from concertina to triangular mode and finally gets distorted before the time pulse of 480 μs completes.

From Table 4, it is also observed that maximum energy absorption is obtained under low-velocity impact case, irrespective of the notch size and configuration. The highest peak load reduction among all the 9 shells is seen in the shell P4 (52.32%), while the least reduction in energy absorption is observed in shell P6 (18.4%). Further, theory of two critical velocity V_{c1} and V_{c2} seems to be verifying from the final deformed shape of shells. The shells under an impact velocity of 20 m/s are deformed completely in the concertina mode, V_i being in between V_{c1} and V_{c2}. While the shells impacting with a velocity of 9 m/s are creating the initial buckle around the buckling triggers provided, V_i being less than V_{c1}. And the final deformed shape of shell P9 is completely distorted, when impacted with a velocity of 40 m/s, V_i being greater than V_{c2}.

On further investigation, it was found that peak load and its reduction is affected by the stress concentration in the shell. The stress concentration and the equivalent plastic strain are accumulated along the line joining the mid-points of notches. The localisation of plastic strain near the notch corner leads to the initiation of buckle at mid-length of shell. Smaller the distance between adjacent notches, larger is the plastic strain localisation as well as the stress concentration, and concertina mode of deformation is obtained, which leads to minimum peak collapse load and maximum reduction in peak load as compared to the cylinder without notches, and vice-versa. The stress concentration around the notch area also have significant effect on the rupturing of

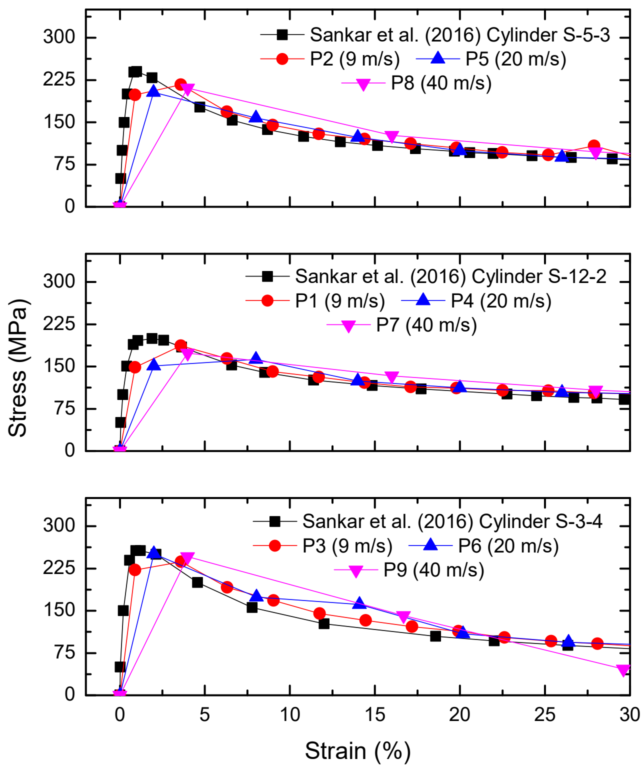

Fig. 6. Nominal stress-strain response of S5-3, S12-2 and S3-4 configuration of shell specimen

shell around the notch. This rupture of shell material is observed in case of circular-hole pattern, around the holes due to concentration of stress, in the experimental study of Sankar et al. [30]. Such rupture is not observed in the present numerical study for diamond-notch pattern.

5. Conclusions

Herein, an attempt is made to numerically investigate the axial deformation of cylindrical shells under higher strain rates using buckling triggers. The buckling triggers used in the study are diamond-notch, and these are compared with circular-hole provided by Sankar et al. [30] in terms of peak collapse load and energy absorption characteristics. Detailed FE analysis is carried out on an aluminium Al 6061-T6 alloy shell to study the initial buckling response under dynamic loading using SHPB setup.

On comparing the two cut-out shapes, it is found that diamond-notch is superior than circular-hole, in terms of peak load reduction and energy efficiency. Also, the net-section perimeter of diamond-notch shell is significantly lesser than that of the circular-hole shell, making each shell lighter in weight by 3.5%. Here, the best yielding configuration is found to be S12-2. Further, on comparing shells under different impact velocities, the theory of two critical velocities is also verified. The set of shells under the impact velocity of 20 m/s is found out to be significant set in terms of peak load reduction and energy efficiency, except the shell P6 which behaved completely in a different manner. Despite the low energy absorption of the shells with notches, the energy efficiency of each shell is higher than the shell without notches.

Disclosures

Free Access to this article is sponsored by SARL ALPHA CRISTO INDUSTRIAL.

References

1. Abramowicz W, Jones N. Dynamic axial crushing of square tubes. International Journal of Damage Mechanics. 1984; 2(2):179–208.

2. Abramowicz W, Jones N. Dynamic axial crushing of circular tubes. International Journal of Impact Engineering. 1984; 2(3): 263–81.

3. Abramowicz W, Jones N. Dynamic progressive buckling of circular and square tubes. International Journal of Impact Engineering. 1986; 4(4): 243–70.

4. Abramowicz W, Jones N. Transition from initial global bending to progressive buckling of tubes loaded statically and dynamically. International Journal of Impact Engineering. 1997; 19(5–6): 415–37.

5. Wang R, Han M, Huang Z, Yang Q. An experimental study on the dynamic axial plastic buckling of cylindrical shells. International Journal of Impact Engineering. 1983; 1: 249–51.

6. Langseth M, Hopperstad OS. Static and dynamic axial crushing of square thin-walled aluminium extrusions. International Journal of Impact Engineering. 1996; 18(7–8): 949–68.

7. Karagiozova D, Jones N. Dynamic elastic-plastic buckling of circular cylindrical shells under axial impact. International Journal of Solids and Structures. 2000; 37: 2005–34.

8. Karagiozova D, Alves M, Jones N. Inertia effects in axisymmetrically deformed cylindrical shells under axial impact. International Journal of Impact Engineering. 2000; 24(10):1083–115.

9. Karagiozova D, Jones N. Influence of stress waves on the dynamic progressive and dynamic plastic buckling of cylindrical shells. International Journal of Solids and Structures. 2001; 38(38–39): 6723–49.

10. Karagiozova D, Jones N. Dynamic effects on buckling and energy absorption of cylindrical shells under axial impact. Thin-Walled Structures. 2001; 39(7): 583–610.

11. Chung Kim Yuen S, Nurick GN. The energy-absorbing characteristics of tubular structures with geometric and material modifications: An overview. Applied Mechanics Reviews. 2008; 61(1–6): 0208021–02080215.

12. Starnes JHJ. Effect of a circular hole on the buckling of cylindrical shells loaded by axial compression. AIAA Journal. 1972; 10(11): 1466–73.

13. Stranes JHJ. Effect of a slot on the buckling load of a cylindrical shell with a circular cutout. AIAA Journal. 1972; 10(2): 227–9.

14. Gupta NK, Gupta SK. Effect of annealing, size and cut-outs on axial collapse behaviour of circular tubes. International Journal of Mechanical Science. 1993; 35(7): 597–613.

15. Lee S, Hahn C, Rhee M, Oh JE. Effect of triggering on the energy absorption capacity of axially compressed aluminum tubes. Materials and Design. 1999; 20(1): 31–40.

16. Mamalis AG, Manolakos DE, Spentzas KN, Ioannidis MB, Koutroubakis S. The effect of the implementation of circular holes as crush initiators to the crushing characteristics of mild steel square tubes: experimental and numerical simulation. International Journal of Crashworthiness. 2009; 14(5): 489-501.

17. Han H, Cheng J, Taheri F, Pegg N. Numerical and experimental investigations of the response of aluminum cylinders with a cutout subject to axial compression. Thin-Walled Structures. 2006; 44(2): 254–70.

18. Shariati M, Rokhi MM. Numerical and experimental investigations on buckling of steel cylindrical shells with elliptical cutout subject to axial compression. Thin-Walled Structures. 2008; 46: 1251–61

19. Huang MY, Tai YS, Hu HT. Dynamic crushing characteristics of high strength steel cylinders with elliptical geometric discontinuities. Theoretical and Applied Fracture Mechanics. 2010; 54: 44–53.

20. Bodlani SB, Chung Kim Yuen S, Nurick GN. The energy absorption characteristics of square mild steel tubes with multiple induced circular hole discontinuities-Part I: Experiments. Journal of Applied Mechanics. 2009; 76(July): 1–11.

21. Bodlani SB, Chung Kim Yuen S, Nurick GN. The energy absorption characteristics of square mild steel tubes with multiple induced circular hole discontinuities-Part II: Numerical simulations. Journal of Applied Mechanics. 2009; 76: 1–10.

22. Arnold B, Altenhof W. Experimental observations on the crush characteristics of AA6061 T4 and T6 structural square tubes with and without circular discontinuities. International Journal of Crashworthiness. 2004; 9(1): 73–87.

23. Ming L, Ren W, Mingbao H. An Experimental investigation of the dynamic axial buckling of cylindrical shells using a Kolsky bar. Acta Mech Sin. 1994; 10(3).

24. Karagiozova D, Jones N. Stress wave effects on the dynamic axial buckling of cylindrical shells under impact. In: Jones N. et al., editors. Proceedings of the Fifth International Conference on Structures under Shock and Impact. Thessaloniki, Greece, Southampton, UK and Boston, USA: Computational Mechanics Publications. 1998; 201-11.

25. Goel MD. Numerical investigation of the axial impact loading behaviour of single, double and stiffened circular tubes. International Journal of Crashworthiness. 2015; 21(1): 41–50.

26. Goel, MD, Laxminarayan K. Deformation and energy absorption of aluminum foam filled square tubes, Advanced Materials Research, Trans Tech Publications, Switzerland, 2012; 585: 34-38.

27. Goel, MD. Deformation, energy absorption and crushing behavior of single-, double- and multi -wall foam filled square and circular tubes, Thin-Walled Structures. 2015; 90: 1-11.

28. Pandarkar A, Goel MD, Hora MS. Axial crushing of hollow and foam filled tubes: an overview, Sadhana, 2016: 1–13. doi:10.1007/s12046-016-0525-4.

29. Goel MD, Pandharkar A, Hora MS. Numerical simulation of crushing and energy absorption behavior of twisted tubes under impact loading, Procedia Engineering, 2017; 173:1365 – 1373.

30. Sankar HR, Parameswaran V. Effect of multiple holes on dynamic buckling of stubby shells: An experimental and

numerical investigation. International Journal of Impact Engineering. 2016; 96: 129–45.

31. ABAQUS, Abaqus/CAE User's Manual, Dassault Systèmes, Providence, RI, 2014.

32. Cheng Q, Altenhof W, Li L. Experimental investigations on the crush behaviour of AA6061-T6 aluminum square tubes with different types of through-hole discontinuities. Thin-Walled Structures. 2006; 44: 441–54.

33. Lesuer DR, Kay GJ, LeBlanc MM. Modeling large strain, high rate deformation in metals. Technical report UCRL-JC-134118, Lawrence Livermore National Laboratory, 2001.